

Article

Adamantane-Isothiourea Hybrid Derivatives: Synthesis, Characterization, In Vitro Antimicrobial, and In Vivo Hypoglycemic Activities

Lamya H. Al-Wahaibi ¹, Hanan M. Hassan ², Amal M. Abo-Kamar ^{2,3}, Hazem A. Ghabbour ⁴ and Ali A. El-Emam ^{4,*}

¹ Department of Chemistry, College of Sciences, Princess Nourah Bint Abdulrahman University, Riyadh 11671, Saudi Arabia; lamya-alwahaibi@hotmail.com

² Department of Pharmaceutical Sciences, College of Pharmacy, Princess Nourah Bint Abdulrahman University, Riyadh 11671, Saudi Arabia; hananhafila@hotmail.com (H.M.H.); amabokamer@pnu.edu.sa (A.M.A.-K.)

³ Department of Microbiology, Faculty of Pharmacy, Tanta University, Tanta, Egypt

⁴ Department of Pharmaceutical Chemistry, College of Pharmacy, King Saud University, Riyadh 11671, Saudi Arabia; ghabbourh@yahoo.com

* Correspondence: aelemam@ksu.edu.sa; Tel.: +966-11-467-7350; Fax: +966-11-467-6220

Academic Editor: Diego Muñoz-Torrero

Received: 14 April 2017; Accepted: 27 April 2017; Published: 29 April 2017

Abstract: A new series of adamantane-isothiourea hybrid derivatives, namely 4-arylmethyl (Z)-N'-(adamantan-1-yl)-morpholine-4-carbothioimidates **7a–e** and 4-arylmethyl (Z)-N'-(adamantan-1-yl)-4-phenylpiperazine-1-carbothioimidates **8a–e** were prepared via the reaction of N-(adamantan-1-yl)morpholine-4-carbothioamide **5** and N-(adamantan-1-yl)-4-phenylpiperazine-1-carbothioamide **6** with benzyl or substituted benzyl bromides, in acetone, in the presence of anhydrous potassium carbonate. The structures of the synthesized compounds were confirmed by ¹H-NMR, ¹³C-NMR, electrospray ionization mass spectral (ESI-MS) data, and X-ray crystallographic data. The in vitro antimicrobial activity of the new compounds was determined against certain standard strains of pathogenic bacteria and the yeast-like pathogenic fungus *Candida albicans*. Compounds **7b**, **7d** and **7e** displayed potent broad-spectrum antibacterial activity, while compounds **7a**, **7c**, **8b**, **8d** and **8e** were active against the tested Gram-positive bacteria. The in vivo oral hypoglycemic activity of the new compounds was carried on streptozotocin (STZ)-induced diabetic rats. Compounds **7a**, **8ab**, and **8b** produced potent dose-independent reduction of serum glucose levels, compared to the potent hypoglycemic drug gliclazide.

Keywords: synthesis; adamantane; isothiourea; carbothioimide; antimicrobial activity; hypoglycaemic activity

1. Introduction

The adamantane nucleus was recognized early as an essential pharmacophore in various pharmacologically-active drugs. The incorporation of an adamantyl moiety into various bioactive molecules results in compounds with relatively high lipophilicity which, in turn, modifies the bioavailability and modulates their therapeutic efficacies [1,2]. Amantadine, the first adamantane-based drug, was approved for the treatment of Influenza A infection [3–5] and as an anti-Parkinsonian drug [6]. Further studies based on amantadine resulted in the development of the potent antiviral drugs rimantadine [7] and tromantadine [8]. Numerous adamantane-based analogues were proved to possess significant inhibitory activity against human immunodeficiency viruses (HIV) [9–12]. The synthetic retinoid derivative CD437 was developed as a potent inducer of apoptosis in human head and neck squamous cell carcinoma [13]. Potent bactericidal and fungicidal activities were reported for several

adamantane derivatives, including SQ109, which was approved for use against drug-susceptible and drug-resistant TB strains [14]. SQ109 also showed excellent inhibitory activity against *Helicobacter pylori*-related duodenal ulcers and carcinomas, and *Candida glabrata* [15]. The adamantane-based drugs, vildagliptin [16], and saxagliptin [17] are currently used as oral hypoglycemic agents for the treatment of type 2 diabetes acting via inhibition of dipeptidyl peptidase IV (DPP-IV). Moreover, the adamantane derivatives MK-544 [18], PF-877423 [19], and AZD6925 [20] were recently developed as 11 β -hydroxysteroid dehydrogenase type 1 (11 β -HSD1) inhibitors as drug candidates for the treatment of non-insulin-dependent diabetes and obesity [21] (Figure 1).

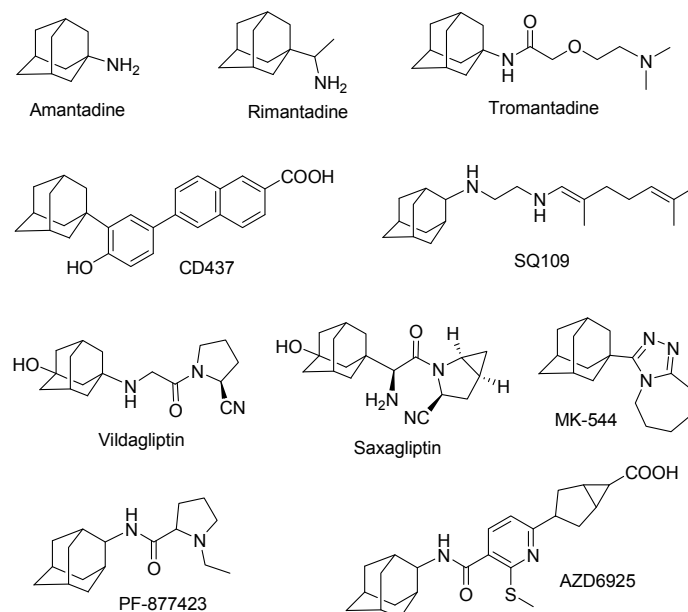


Figure 1. Biologically-active adamantane-based derivatives.

On the other hand, several compounds containing an isothiourea moiety were reported to possess significant antiviral [22], histamine-H₃ antagonistic [23,24], calcium channel antagonistic [25], anticancer [26], antibacterial [27], and nitric oxide synthase inhibitory [28,29] activities.

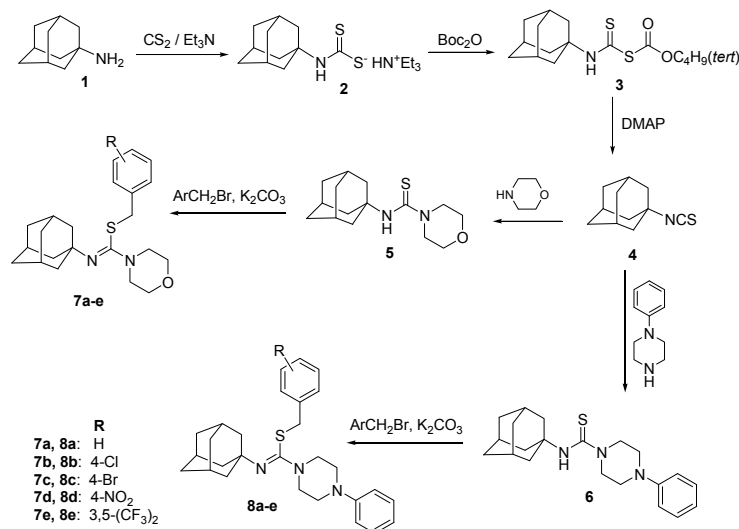
In view of the diverse pharmacological properties of adamantane and isothiourea derivatives, and following our previous studies on the chemical and biological properties of adamantane derivatives [10,30–33], we report herein the synthesis and characterization of novel adamantane derivatives containing an isothiourea moiety as potential antimicrobial and/or hypoglycemic agents.

2. Results and Discussion

2.1. Chemical Synthesis

The key starting material 1-adamantyl isothiocyanate **4** was prepared in good yield via our previously described methods [33]. The reaction of 1-adamantylamine **1** with carbon disulphide and trimethylamine, in ethanol, yielded the dithiocarbamate salt **2**, which was reacted with di-*tert*-butyl dicarbonate (Boc₂O) to yield the intermediate **3**. The intermediate **3** was stirred with catalytic amount of 4-dimethylaminopyridine (DMAP) to furnish the target product **4**. The reaction of 1-adamantyl isothiocyanate **4** with morpholine and 1-phenylpiperazine, in boiling ethanol, yielded the corresponding *N*-(adamantan-1-yl)morpholine-4-carbothioamide **5** and *N*-(adamantan-1-yl)-4-phenylpiperazine-1-carbothioamide **6**, respectively [33]. The carbothioamides **5** and **6** were reacted with benzyl or substituted benzyl bromides, in acetone, in the presence of anhydrous potassium carbonate to yield the corresponding *S*-arylmethyl derivatives **7a–e** and **8a–e**, respectively, in good yields (Scheme 1, Table 1). The structures of the target compounds **7a–e** and **8a–e** were confirmed by

elemental analyses (Table S1), in addition to the $^1\text{H-NMR}$ and $^{13}\text{C-NMR}$, and electrospray ionization mass spectral (ESI-MS) data, which were in full agreement with their structures. The ESI-MS data showed the correct positive ions $(\text{M} + \text{H})^+$ ions for all compounds. In addition, compounds **7d** and **8d** were subjected to single crystal X-ray studies.



Scheme 1. Synthetic approach for the target compounds **7a–e** and **8a–e**.

Table 1. Crystallization solvents, melting points, yield percentages, molecular formulae, and molecular weights of compounds **7a–e** and **8a–e**.

Comp. No.	R	Cryst. Solv.	M.p. (°C)	Yield (%)	Mol. Formula (Mol. Wt.)
7a	H	EtOH/H ₂ O	108–110	91	C ₂₂ H ₃₀ N ₂ OS (370.55)
7b	4-Cl	EtOH	92–94	76	C ₂₂ H ₂₉ ClN ₂ OS (405.0)
7c	4-Br	EtOH	98–100	85	C ₂₂ H ₂₉ BrN ₂ OS (449.45)
7d	4-NO ₂	EtOH	118–120	95	C ₂₂ H ₂₉ N ₃ O ₃ S (415.55)
7e	3,5-(CF ₃) ₂	EtOH/H ₂ O	106–108	72	C ₂₄ H ₂₈ F ₆ N ₂ OS (506.55)
8a	H	EtOH/H ₂ O	137–139	88	C ₂₈ H ₃₅ N ₃ S (445.66)
8b	4-Cl	EtOH	153–155	90	C ₂₈ H ₃₄ ClN ₃ S (480.11)
8c	4-Br	EtOH	140–142	92	C ₂₈ H ₃₄ BrN ₃ S (524.56)
8d	4-NO ₂	EtOH	145–147	96	C ₂₈ H ₃₄ N ₄ O ₂ S (490.66)
8e	3,5-(CF ₃) ₂	EtOH/H ₂ O	113–115	75	C ₃₀ H ₃₃ F ₆ N ₃ S (581.66)

2.2. Crystallographic Studies

The single crystal X-ray crystallographic data of compounds **7d** and **8d** are summarized in Table 2. Compound **7b** crystallizes in the centrosymmetric monoclinic space group $P2_1/c$ with one molecule in the asymmetric unit ($Z = 4$). The ORTEP (Oak Ridge Thermal Ellipsoid Plot) is shown in Figure 2. The morpholine ring adopts a chair conformation and the mean planes of the nitrophenyl and morpholine rings make a dihedral angle of 52.55 (5). The conformation about the N1=C11 imine bond is *Z* (*cis*) configuration. The crystal packing is mainly controlled by intermolecular C-H...O hydrogen bonding (Figure 3).

Table 2. Single-crystal X-ray crystallographic data of compounds **7d** and **8d**.

Data	Compound 7d	Compound 8d
Formula	C ₂₂ H ₂₉ N ₃ O ₃ S	C ₂₈ H ₃₄ N ₄ O ₂ S
Formula weight	415.55	490.66
Temperature (K)	293	293
Wavelength (Å)	0.71073	0.71073
Crystal system	Monoclinic	Orthorhombi

Table 2. Cont.

Data	Compound 7d	Compound 8d
Space group	$P2_1/c$	$P2_12_12_1$
a, b, c (Å)	6.9204 (5), 29.775 (3), 10.2725 (10)	6.9426 (9), 9.6472 (12), 39.086 (5)
V (Å ³)	2116.7 (3)	2617.8 (6)
Z	4	4
Radiation type	Mo $K\alpha$	Mo $K\alpha$
μ (mm ⁻¹)	0.18	0.16
No. of reflections	11033	25091
No. of unique reflections/obs. reflections	3718/2253	4609/1447
No. of parameters	262	318
No. of restraints	0	0
$\Delta\rho_{\max}, \Delta\rho_{\min}$ (e Å ⁻³)	0.28, -0.21	0.44, -0.40
T_{\min}, T_{\max}	0.939, 0.989	0.924, 0.957
R_{int}	0.073	0.526
Crystal size (mm)	0.35 × 0.11 × 0.06	0.85 × 0.21 × 0.05
$R[F^2 > 2\sigma(F^2)], wR(F^2), S$	0.052, 0.192, 0.65	0.128, 0.296, 1.02
CCDC number	1525183	1523432

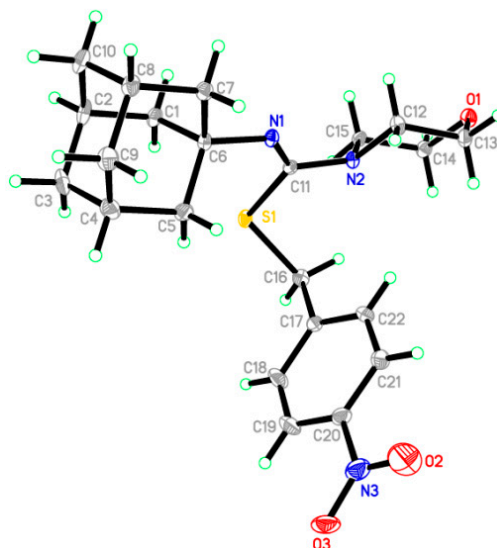


Figure 2. ORTEP diagram of compound 7d drawn at 40% ellipsoids for non-hydrogen atoms.

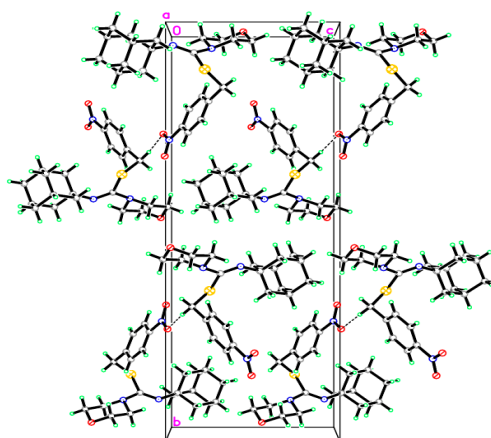


Figure 3. Molecular packing of compound 7d viewed hydrogen bonds, which are drawn as dashed lines.

Compound **8b** crystallizes in the orthorhombic space group $P2_12_12_1$ with one molecule in the asymmetric unit ($Z = 4$). The ORTEP is shown Figure 4. The piperazine ring also adopts a chair conformation with a dihedral angle of 39.25 (4). The conformation about the N1A=C11A imine bond is *Z* (*cis*) configuration. The crystal packing is mainly controlled by intermolecular C-H...S hydrogen bonding (Figure 5).

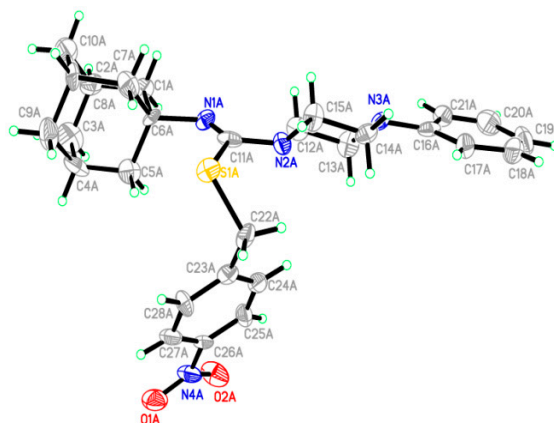


Figure 4. ORTEP diagram of compound **8d** drawn at 40% ellipsoids for non-hydrogen atoms.

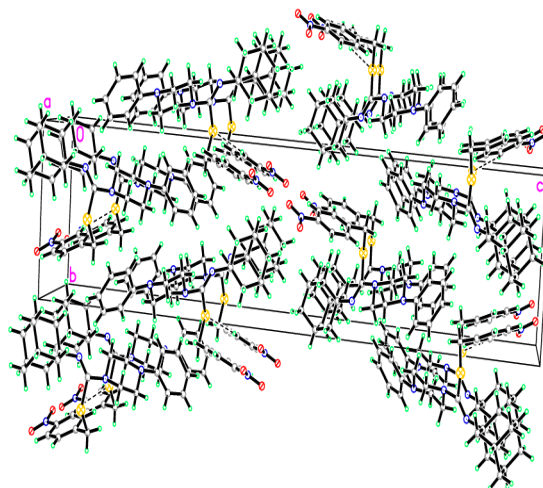


Figure 5. Molecular packing of compound **8d** viewed hydrogen bonds, which are drawn as dashed lines.

2.3. In Vitro Antimicrobial Activity

The newly synthesized compounds **7a–e** and **8a–e** were tested for their in vitro growth inhibitory activity against the standard bacterial strains of the American type culture collection ATCC, *Staphylococcus aureus* ATCC 6571, *Bacillus subtilis* ATCC 5256, *Micrococcus luteus* ATCC 27141 (Gram-positive bacteria), *Escherichia coli* ATCC 8726, *Pseudomonas aeruginosa* ATCC 27853 (Gram-negative bacteria), and the yeast-like pathogenic fungus *Candida albicans* MTCC 227. The preliminary antimicrobial activity testing was carried out using the semi-quantitative agar-disc diffusion method with Müller-Hinton agar medium [34]. The outcomes of the preliminary antimicrobial screening of compounds **7a–e**, **8a–e** (200 µg/disc), the antibacterial antibiotics gentamicin sulphate, ampicillin trihydrate and the antifungal drug clotrimazole (100 µg/disc) and the calculated log *P* values (Clog *P*) of the tested compounds (calculated using the CS ChemOffice Ultra version 8.0, CambridgeSoft, Cambridge, MA, USA), are shown in Table 3.

The main features of the results of the antimicrobial activity testing revealed that the tested compounds generally displayed marked antibacterial and marginal antifungal activities against the tested microorganisms, the antibacterial activity against the Gram-positive bacteria was higher than the activity against the Gram-negative bacteria, and the compound lipophilicity had no influence on their activity. In addition, the Gram-positive bacteria *S. aureus* and *B. subtilis* are more sensitive than *M. luteus*, and the Gram-negative bacteria *P. aeruginosa* was more resistant than *E. coli*. Potent antibacterial activity was shown by compounds **7a–e**, **8d** and **8e** which produced growth inhibition zones ≥ 20 mm against one or more of the tested microorganisms. In the morpholine derivatives **7a–e**, compounds **7b**, **7d** and **7e** retained good broad spectrum antibacterial activity; while compound **7a** displayed good activity against the Gram-positive bacteria and medium activity against *E. coli* (inhibition zones 15–19 mm). The optimum activity was achieved by **7e** which was highly active against all the tested bacterial strains. In the piperazine derivatives **8a–c**, compounds **8b**, **8d** and **8e** showed high activity against the tested Gram-positive bacteria, while compounds **8a** and **8c** showed medium activity against the tested Gram-positive bacteria and weak activity (growth inhibition zones 10–14 mm) against the tested Gram-negative bacteria. The activity against yeast-like pathogenic fungus *C. albicans* of the tested compounds was rather lower than that against the tested bacterial strains. Compound **8d** showed medium inhibitory activity, compounds **7b**, **7d**, **8a**, **8b**, **8c** and **8e** displayed weak activity and compounds **7a**, **7c** and **7e** were practically inactive (growth inhibition zones < 10 mm).

Table 3. Antimicrobial activity of compounds **7a–e** and **8a–e** (200 $\mu\text{g}/8$ mm disc), the broad-spectrum antibacterial drugs gentamicin sulphate, ampicillin trihydrate and the antifungal drug clotrimazole (100 $\mu\text{g}/8$ mm disc) against *Staphylococcus aureus* ATCC 6571 (SA), *Bacillus subtilis* ATCC 5256 (BS), *Micrococcus luteus* ATCC 27141 (ML), *Escherichia coli* ATCC 8726 (EC), *Pseudomonas aeruginosa* ATCC 27853 (PA), and the yeast-like pathogenic fungus *Candida albicans* MTCC 227 (CA).

Comp. No.	Clog P	Diameter of Growth Inhibition Zone (mm) ^a					
		SA	BS	ML	EC	PA	CA
7a	5.584	22 (2) ^b	21 (4) ^b	20 (4) ^b	18 (16) ^b	14 (64) ^b	-
7b	6.297	24 (4) ^b	28 (0.5) ^b	22 (4) ^b	22 (20) ^b	15 (32)	11 (>128) ^b
7c	6.447	22 (4) ^b	18 (16) ^b	14 (64) ^b	13 (128) ^b	12 (128) ^b	-
7d	5.327	31 (0.5) ^b	32 (0.25) ^b	28 (0.5) ^b	22 (1) ^b	18 (4) ^b	14 (32) ^b
7e	7.350	33 (0.25) ^b	34 (0.25) ^b	28 (1) ^b	24 (2) ^b	20 (4) ^b	-
8a	7.130	18 (8) ^b	18 (8) ^b	14 (128) ^b	12 (>128) ^b	10 (>128) ^b	10 (>128) ^b
8b	7.843	21 (8) ^b	24 (2) ^b	16 (32) ^b	16 (64) ^b	12 (>128) ^b	13 (64) ^b
8c	7.993	17 (32) ^b	19 (8) ^b	14 (64) ^b	11 (>128) ^b	10 (>128) ^b	12 (128) ^b
8d	6.873	24 (1) ^b	28 (1) ^b	20 (2) ^b	18 (2) ^b	14 (4) ^b	16 (16) ^b
8e	8.896	28 (1) ^b	31 (0.5) ^b	22 (2) ^b	19 (4) ^b	18 (8) ^b	14 (64) ^b
Gentamicin sulfate		27 (1) ^b	26 (2) ^b	20 (2) ^b	22 (0.5) ^b	21 (0.5) ^b	NT
Ampicillin trihydrate		22 (2) ^b	23 (1) ^b	20 (2) ^b	16 (8) ^b	16 (8) ^b	NT
Clotrimazole		NT	NT	NT	NT	NT	21 (4) ^b

^a (-): inactive (inhibition zone < 10 mm), ^b Figures shown in parentheses represent the MIC values ($\mu\text{g}/\text{mL}$), NT: not tested.

From the above results, it could be concluded that the antibacterial activity of the morpholine derivatives **7a–e** is generally superior to their *N*-phenylpiperazine analogues. In addition, the presence of the electron-withdrawing substituents NO_2 and CF_3 (compounds **7d**, **7e**, **8d** and **8e**) greatly enhanced the antibacterial activity. Unlike the antibacterial activity, the *N*-phenylpiperazine analogues **8a–e** were generally more active than the morpholine analogues **7a–e** against *C. albicans*. The values of the minimal inhibitory concentration (MIC) in Müller-Hinton Broth [35] for the tested compounds (Table 3) were correlated to the results obtained in the preliminary screening.

2.4. In Vivo Hypoglycemic Activity

The oral hypoglycaemic activity of compounds **7a–c** and **8a–c** was determined in streptozotocin (STZ)-induced diabetic rats. STZ induces its hyperglycemic activity via irreversible damage to the

pancreatic beta cells, resulting in loss of insulin secretion [36,37]. The compounds were tried in 10 and 20 mg/kg dose levels. The dose levels (10 and 20 mg/kg) were determined after pilot experiments which showed that increasing the dose to 30 mg/kg was found to produce toxic central nervous manifestations in the form of severe symmetric convulsions. The hypoglycemic activity testing experiment (animal treatments, induction of experimental diabetes, and measurement of serum glucose level) was carried out following the previously reported protocols [32,33]. The results of the oral hypoglycemic activity of compounds **7a–c**, **8a–c** (10 and 20 mg/kg), and the potent hypoglycemic drug gliclazide in STZ-induced diabetic rats (10 mg/kg) are shown in Table 4.

The optimum hypoglycemic activity was attained by compounds **7a**, **8a**, and **8b** which produced potent dose-independent reduction of serum glucose levels, compared to gliclazide at 10 mg/kg dose level (Potency ratio 71.08, 75.13 and 79.04%, respectively). Compound **7b** showed medium dose-dependent hypoglycemic activity and compound **8c** showed weak activity at 10 mg/kg dose level without significant increase in the activity at 20 mg/kg dose level. Despite the high activity of the bis(3,5-trifluoromethyl) derivative **7e** (Potency ratio 82.32%), increasing the dose produced toxic central nervous manifestations. Similarly, compound **8e** showed toxic manifestations at 10 and 20 mg/kg doses.

The hypoglycemic activity of the tested compounds revealed that the piperazine derivatives **8a–e** are generally more active than their morpholine analogues **7a–e**. In addition, the aryl substituents greatly influenced the hypoglycemic activity and toxicity. The optimum activity was attained by the phenyl derivatives (**7a**, **8a**) and to a lesser extent the chlorophenyl derivatives (**7b**, **8b**). The bis(3,5-trifluoromethyl) derivatives were generally toxic.

Table 4. Oral hypoglycemic activity of compounds **7a–c**, **8a–c** (10 and 20 mg/kg), and gliclazide (10 mg/kg) in STZ-induced diabetic rats.

Treatment	Results		
	C ₀ (mg/dL) ^a	C ₂₄ (mg/dL) ^a	% Glucose Reduction ^b
Group 1 ^c	302.8 ± 11.64	290.2 ± 18.22	4.16%
Group 1 ^d	299.2 ± 16.50	171.6 ± 12.32 *	42.65%
7a (10 mg/kg)	304.8 ± 13.26	212.4 ± 12.16 *	30.31% (71.08)
7a (20 mg/kg)	300.6 ± 11.65	134.6 ± 9.75 *	55.22% (64.74)
7b (10 mg/kg)	288.9 ± 12.15	245.2 ± 19.25 *	15.13% (35.47)
7b (20 mg/kg)	294.8 ± 9.08	201.5 ± 9.60 *	31.65% (37.13)
7c (10 mg/kg)	284.8 ± 19.55	281.2 ± 7.19	1.26% (2.69)
7c (20 mg/kg)	290.2 ± 21.64	286.8 ± 19.02	2.75% (1.37)
7d (10 mg/kg)	278.1 ± 16.24	282.2 ± 27.20	−1.47%
7d (20 mg/kg)	302.6 ± 22.25	299.8 ± 18.80	0.93% (1.08)
7e (10 mg/kg)	306.2 ± 15.20	198.7 ± 19.10 *	35.12 (82.32)
7e (20 mg/kg)		Toxic	
8a (10 mg/kg)	294.6 ± 11.30	200.2 ± 9.88 *	32.04% (75.13)
8a (20 mg/kg)	290.6 ± 8.60	108.4 ± 11.05 *	62.70% (73.50)
8b (10 mg/kg)	301.4 ± 9.06	199.8 ± 10.01 *	33.71% (79.04)
8b (20 mg/kg)	296.0 ± 11.02	144.6 ± 10.01 *	51.15% (59.96)
8c (10 mg/kg)	320.5 ± 22.05	277.6 ± 16.20	13.39% (31.38)
8c (20 mg/kg)	313.5 ± 18.60	269.9 ± 20.12	13.91% (16.30)
8d (10 mg/kg)	295.0 ± 22.45	289.2 ± 25.28	1.97% (4.61)
8d (20 mg/kg)	304.5 ± 27.50	309.0 ± 25.95	−1.48
8e (10 mg/kg)	286.6 ± 13.22	178.2 ± 16.04 *	37.82% (88.68)
8e (20 mg/kg)		Toxic	

^a Results are expressed as mean ± S.E.M. (*n* = 5), ^b The figures shown in parentheses are the relative potency compared with gliclazide, ^c Treated with a single oral dose of 0.5% (*w/v*) aqueous CMC solution (5 mL/kg), ^d Treated with 10 mg/kg gliclazide in 0.5% (*w/v*) aqueous CMC, * Significant difference at *p* < 0.01 compared with the corresponding control.

3. Materials and Methods

3.1. General

Melting points (°C, uncorrected) were measured in open glass capillaries using a Branstead 9100 electrothermal melting point apparatus (Thermo Fisher Scientific, Waltham, MA, USA). Nuclear magnetic resonance (NMR) spectra were obtained on a Bruker Ascend 700 NMR spectrometer (Fällanden, Switzerland) at 700.17 MHz for ^1H and 176.08 MHz for ^{13}C , using CDCl_3 as the solvent. The chemical shifts are expressed in δ (ppm) downfield from tetramethylsilane (TMS) as internal standard, coupling constants (J) are expressed in Hz. Electrospray ionization mass spectra (ESI-MS) were recorded on an Agilent 6410 Triple Quad tandem mass spectrometer (Agilent Technologies, Santa Clara, CA, USA) at 4.0 kV for positive ions. Elemental analyses (C, H, N, and S) were in agreement with the proposed structures within $\pm 0.4\%$ of the theoretical values (Table S1). Monitoring the reactions and checking the purity of the final products were carried out by thin layer chromatography (TLC) using silica gel precoated aluminum sheets (60 F_{254} ; Merck Schuchardt, Darmstadt, Germany), and visualization with ultraviolet light (UV) at 365 and 254 nm. The reference drugs gentamicin sulfate (CAS 1405-41-0), ampicillin trihydrate (CAS 7177-48-2), clotrimazole (CAS 23593-75-1) and gliclazide (CAS 21187-98-4), and streptozotocin (CAS 18883-66-4) were purchased from Sigma-Aldrich Chemie GmbH, Taufkirchen, Germany. The Sprague-Dawley rats were purchased from local animal house. The commercial glucose oxidase (GO) assay kit (Sigma-Aldrich Co., St. Louis, MO, USA) were used for measurement of serum glucose levels. The animal experiments for the determination of the hypoglycemic activity were performed in accordance with the guidelines provided by the Experimental Animal Laboratory (EAL) and approved by the Animal Care and Use Committee (ACUC) of the College of Pharmacy, King Saud University (Saudi Arabia). The X-ray crystallographic data of compound **8c** was recently described [38].

3.2. Synthesis of 4-Arylmethyl (Z)-N'-(Adamantan-1-yl)-Morpholine-4-Carbothioimidates **7a–e** and 4-Arylmethyl (Z)-N'-(Adamantan-1-yl)-4-Phenylpiperazine-1-Carbothioimidates **8a–e**

The appropriate arylmethyl bromide (2 mmol) and anhydrous potassium carbonate (276 mg, 2 mmol) were added to a solution of *N*-(adamantan-1-yl)morpholine-4-carbothioamide **5** (560 mg, 2 mmol) or *N*-(adamantan-1-yl)-4-phenylpiperazine-1-carbothioamide **6** (711 mg, 2 mmol), in anhydrous acetone (15 mL), and the mixture was heated under reflux for 4 h. The solvent was then distilled off in vacuo and the resulting residues were washed with water (20 mL), dried, and crystallized from ethanol or aqueous ethanol.

Benzyl (Z)-N'-(adamantan-1-yl)-morpholine-4-carbothioimide **7a**: $^1\text{H-NMR}$: δ 1.61–1.66 (m, 6H, adamantane-H), 1.85 (m, 6H, adamantane-H), 2.0 (s, 3H, adamantane-H), 3.20–3.21 (m, 4H, morpholine-H), 3.65–3.72 (m, 4H, morpholine-H), 3.90 (s, 2H, benzylic CH_2), 7.07–7.19 (m, 5H, Ar-H). $^{13}\text{C-NMR}$: δ 29.02, 29.80, 35.96, 54.18 (adamantane-C), 37.06 (benzylic CH_2), 49.66, 66.42 (morpholine-C), 125.60, 126.44, 127.90, 140.02 (Ar-C), 154.46 (C=N). ESI-MS, m/z : 372.3 (M + H) $^+$.

4-Chlorobenzyl (Z)-N'-(adamantan-1-yl)-morpholine-4-carbothioimide **7b**: $^1\text{H-NMR}$: δ 1.62–1.65 (m, 6H, adamantane-H), 1.69–1.72 (m, 6H, adamantane-H), 2.05–2.06 (m, 3H, adamantane-H), 3.99 (s, 2H, benzylic CH_2), 3.20–3.22 (m, 4H, morpholine-H), 3.65–3.72 (m, 4H, morpholine-H), 6.99 (d, 2H, Ar-H, $J = 7.5$ Hz), 7.14 (d, 2H, Ar-H, $J = 7.5$ Hz). $^{13}\text{C-NMR}$: δ 29.26, 29.99, 35.98, 54.08 (adamantane-C), 36.98 (benzylic CH_2), 48.60, 66.44 (morpholine-C), 127.65, 128.65, 133.0, 138.04 (Ar-C), 154.24 (C=N). ESI-MS, m/z (Rel. Int.): 405.4 (M + H, 100) $^+$, 407.4 (M + 2 + H, 35) $^+$.

4-Bromobenzyl (Z)-N'-(adamantan-1-yl)-morpholine-4-carbothioimide **7c**: $^1\text{H-NMR}$: δ 1.63–1.69 (m, 6H, adamantane-H), 1.84 (m, 6H, adamantane-H), 2.01 (s, 3H, adamantane-H), 3.25–3.30 (m, 4H, morpholine-H), 3.69–3.74 (m, 4H, morpholine-H), 3.91 (s, 2H, benzylic CH_2), 7.17 (d, 2H, Ar-H, $J = 7.5$ Hz), 7.45 (d, 2H, Ar-H, $J = 7.5$ Hz). $^{13}\text{C-NMR}$: δ 29.59, 29.94, 36.57, 54.69 (adamantane-C), 37.76

(benzylic CH₂), 49.70, 66.85 (morpholine-C), 121.0, 130.51, 137.26, 146.91 (Ar-C), 156.46 (C=N). ESI-MS, *m/z* (Rel. Int.): 449.4 (M + 2 + H, 100)⁺, 451.4 (M + 2 + H, 98)⁺.

4-Nitrobenzyl (Z)-N'-(adamantan-1-yl)-morpholine-4-carbothioimide 7d: ¹H-NMR: δ 1.62 (s, 6H, adamantane-H), 1.77–1.79 (m, 6H, adamantane-H), 1.98–2.0 (m, 3H, adamantane-H), 3.24–3.30 (m, 4H, morpholine-H), 3.69–3.72 (m, 4H, morpholine-H), 4.02 (s, 2H, benzylic CH₂), 7.42 (d, 2H, Ar-H, *J* = 8.2 Hz), 8.21 (d, 2H, Ar-H, *J* = 8.2 Hz). ¹³C-NMR: δ 29.58, 29.84, 36.44, 54.79 (adamantane-C), 37.53 (benzylic CH₂), 49.79, 66.78 (morpholine-C), 123.76, 129.64, 146.07, 146.91 (Ar-C), 156.71 (C=N). ESI-MS, *m/z*: 416.2 (M + H)⁺.

3,5-Bis(trifluoromethyl)benzyl (Z)-N'-(adamantan-1-yl)-morpholine-4-carbothioimide 7e: ¹H-NMR: δ 1.53–1.56 (m, 12H, adamantane-H), 1.85–1.87 (m, 3H, adamantane-H), 3.10–3.12 (m, 4H, morpholine-H), 3.68–3.70 (m, 4H, morpholine-H), 4.17 (s, 2H, benzylic CH₂), 7.95 (s, 1H, Ar-H), 8.0 (s, 2H, Ar-H). ¹³C-NMR: δ 29.16, 29.66, 35.25, 54.85 (adamantane-C), 36.41 (benzylic CH₂), 49.76, 66.20 (morpholine-C), 120.76, 122.72, 130.39, 142.78 (Ar-C), 124.89 (CF₃), 148.37 (C=N). ESI-MS, *m/z*: 507.2 (M + H)⁺.

Benzyl (Z)-N'-(adamantan-1-yl)-4-phenylpiperazine-1-carbothioimide 8a: ¹H-NMR: δ 1.69 (s, 6H, adamantane-H), 1.74 (s, 6H, adamantane-H), 2.0 (s, 3H, adamantane-H), 2.88–2.92 (m, 4H, piperazine-H), 3.02–3.06 (m, 4H, piperazine-H), 3.98 (s, 2H, benzylic CH₂), 6.84–7.04 (m, 5H, Ar-H), 7.12–7.16 (m, 5H, Ar-H). ¹³C-NMR: δ 29.10, 29.96, 35.68, 53.98 (adamantane-C), 46.90, 48.18 (piperazine-C), 36.90 (benzylic CH₂), 114.28, 119.90, 126.92, 128.24, 129.0, 130.58, 139.94, 149.26 (Ar-C), 152.0 (C=N). ESI-MS, *m/z*: 446.3 (M + H)⁺.

4-Chlorobenzyl (Z)-N'-(adamantan-1-yl)-4-phenylpiperazine-1-carbothioimide 8b: ¹H-NMR: δ 1.71–1.76 (m, 12H, adamantane-H), 2.15–2.17 (m, 3H, adamantane-H), 2.63–2.65 (m, 4H, piperazine-H), 3.22–3.24 (m, 4H, piperazine-H), 3.98 (s, 2H, benzylic CH₂), 6.89–6.91 (m, 3H, Ar-H), 6.95–6.96 (m, 2H, Ar-H), 7.29–7.33 (m, 4H, Ar-H). ¹³C-NMR: δ 29.17, 29.71, 35.51, 53.07 (adamantane-C), 48.65, 48.10 (piperazine-C), 36.39 (benzylic CH₂), 115.55, 116.13, 119.89, 128.49, 129.16, 129.45, 130.57, 150.31 (Ar-C), 151.27 (C=N). ESI-MS, *m/z* (Rel. Int.): 380.2 (M + H, 100)⁺, 382.2 (M + 2 + H, 37)⁺.

4-Bromobenzyl (Z)-N'-(adamantan-1-yl)-4-phenylpiperazine-1-carbothioimide 8c: ¹H-NMR: δ 1.65 (s, 6H, adamantane-H), 1.86 (s, 6H, adamantane-H), 2.02–2.03 (m, 3H, adamantane-H), 3.26–3.27 (m, 4H, piperazine-H), 3.43–3.44 (m, 4H, piperazine-H), 3.95 (s, 2H, benzylic CH₂), 6.92–7.93 (m, 1H, Ar-H), 7.00–7.01 (m, 2H, Ar-H), 7.18 (d, 2H, Ar-H, *J* = 7.0 Hz), 7.29–7.33 (m, 2H, Ar-H), 7.44 (d, 2H, Ar-H, *J* = 7.0 Hz). ¹³C-NMR: δ 29.95, 36.58, 42.98, 54.70 (adamantane-C), 48.96, 49.17 (piperazine-C), 37.77 (benzylic CH₂), 116.20, 119.97, 120.94, 129.22, 130.59, 131.54, 137.33, 149.26 (Ar-C), 151.29 (C=N). ESI-MS, *m/z* (Rel. Int.): 524.4 (M + H, 98)⁺, 526.4 (M + 2 + H, 100)⁺ [38].

4-Nitrobenzyl (Z)-N'-(adamantan-1-yl)-4-phenylpiperazine-1-carbothioimide 8d: ¹H-NMR: δ 1.53 (s, 6H, adamantane-H), 1.72 (s, 6H, adamantane-H), 1.91 (s, 3H, adamantane-H), 3.16–3.18 (m, 4H, piperazine-H), 3.30–3.33 (m, 4H, piperazine-H), 3.97 (s, 2H, benzylic CH₂), 6.80–6.89 (m, 3H, Ar-H), 7.18–7.29 (m, 2H, Ar-H), 7.36 (d, 2H, Ar-H, *J* = 8.0 Hz), 8.08 (d, 2H, Ar-H, *J* = 8.0 Hz). ¹³C-NMR: δ 29.65, 29.90, 36.52, 54.86 (adamantane-C), 37.54 (benzylic CH₂), 43.03, 49.12 (piperazine-C), 116.21, 120.05, 123.72, 129.21, 129.66, 146.14, 146.94, 148.09 (Ar-C), 151.22 (C=N). ESI-MS, *m/z*: 491.2 (M + H)⁺.

3,5-Bis(trifluoromethyl)benzyl (Z)-N'-(adamantan-1-yl)-4-phenylpiperazine-1-carbothioimide 8e: ¹H-NMR: δ 1.58 (s, 6H, adamantane-H), 1.69 (s, 6H, adamantane-H), 1.95–1.97 (m, 3H, adamantane-H), 3.29–3.31 (m, 4H, piperazine-H), 3.40–3.42 (m, 4H, piperazine-H), 4.04 (s, 2H, benzylic CH₂), 6.93–7.02 (m, 3H, Ar-H), 7.29 (s, 1H, Ar-H), 7.32–7.34 (m, 2H, Ar-H), 7.78 (s, 2H, Ar-H). ¹³C-NMR: δ 29.80, 35.51, 36.44, 54.80 (adamantane-C), 37.31 (benzylic CH₂), 49.0, 49.13 (piperazine-C), 116.28, 120.12, 129.16, 129.24, 131.44, 131.63, 141.30, 147.50 (Ar-C), 124.04 (CF₃), 151.19 (C=N). ESI-MS, *m/z*: 582.2 (M + H)⁺.

3.3. Crystal Growth and Single Crystal X-ray Study

Single crystals suitable for X-ray analysis were obtained by slow evaporation of CHCl₃:EtOH (1:1; 5 mL) solution of compounds **7d** and **8d** at room temperature. Data were collected on a Bruker APEX-II D8 Venture area diffractometer, equipped with graphite monochromatic Mo K α radiation ($\lambda = 0.71073 \text{ \AA}$) at 100 K. Unit cell measurement, data collection, integration, scaling, and absorption corrections for the crystals were conducted using Bruker Apex II software [39]. Data reduction was done by Bruker SAINT suite [40]. The crystal structures were solved by the full matrix least squares method using SHELXL 2014 [41]. Absorption correction was applied using SADABS program [42]. ORTEP (Oak Ridge Thermal Ellipsoid Plot) was generated using Mercury 3.5.1 Cambridge Crystallographic Data Centre (CCDC) program [43].

4. Conclusions

In this study, new adamantane-linked isothioureia derivatives were synthesized and their in vitro antimicrobial and in vivo hypoglycemic activities were determined. Compounds **7b**, **7d**, and **7e** displayed potent broad-spectrum antibacterial activity, while compounds **7a**, **7c**, **8b**, **8d**, and **8e** were active against the tested Gram-positive bacteria. The tested compounds were generally inactive against the yeast-like pathogenic fungus *Candida albicans*. The in vivo oral hypoglycemic activity of the synthesized compounds was determined in streptozotocin (STZ)-induced diabetic rats. Compounds **7a**, **8a**, and **8b** produced potent dose-independent reduction of serum glucose levels compared to gliclazide at 10 mg/kg dose level (potency ratios of 71.08%, 75.13%, and 79.04%, respectively). The active compounds are considered to be good candidates as newer antibacterial and hypoglycemic agents, though, further studies including toxicity testing and molecular docking for the exploration of the mechanism of their biological activity are required for optimization of the activity which are being undertaken.

Supplementary Materials: Supplementary materials (the experimental details of the determination of in vitro antimicrobial activity, in vivo hypoglycemic activity and microanalytical data) are available online.

Acknowledgments: The authors would like to thank the Deanship of Scientific Research, Princess Nourah Bint Abdulrahman University for funding this study (Research Project No. 37-S-173).

Author Contributions: L.H.A.-W. and A.A.E.-E. synthesized and characterized the target compounds and prepared the single crystals. H.M.H. performed the in vivo hypoglycemic testing, A.M.A.-K. conceived the antimicrobial testing. H.A.G. carried out the X-ray analysis. All authors discussed the contents of the manuscript and approved the submission.

Conflicts of Interest: The authors declare no conflict of interest.

References

1. Liu, J.; Obando, D.; Liao, V.; Lifa, T.; Codd, R. The many faces of the adamantyl group in drug design. *Eur. J. Med. Chem.* **2011**, *46*, 1949–1963. [[CrossRef](#)] [[PubMed](#)]
2. Lamoureux, G.; Artavia, G. Use of the adamantane structure in medicinal chemistry. *Curr. Med. Chem.* **2010**, *17*, 2967–2978. [[CrossRef](#)] [[PubMed](#)]
3. Davies, W.L.; Grunnert, R.R.; Haff, R.F.; McGahen, J.W.; Neumeyer, E.M.; Paulshock, M.; Watts, J.C.; Wood, T.R.; Hermann, E.C.; Hoffmann, C.E. Antiviral activity of 1-adamantamine (amantadine). *Science* **1964**, *144*, 862–863. [[CrossRef](#)] [[PubMed](#)]
4. Togo, Y.; Hornick, R.B.; Dawkins, A.T. Studies on induced influenza in man. I. Double blind studies designed to assess prophylactic efficacy of amantadine hydrochloride against A₂/Rockville/1/65 strain. *J. Am. Med. Assoc.* **1968**, *203*, 1089–1094. [[CrossRef](#)]
5. Wendel, H.A.; Snyder, M.T.; Pell, S. Trial of amantadine in epidemic influenza. *Clin. Pharmacol. Ther.* **1966**, *7*, 38–43. [[CrossRef](#)]
6. Schwab, R.S.; England, A.C.; Poskanzer, D.C.; Young, R.R. Amantadine in the treatment of Parkinson's disease. *J. Am. Med. Assoc.* **1969**, *208*, 1168–1170. [[CrossRef](#)]

7. Rabinovich, S.; Baldini, J.T.; Bannister, R. Treatment of influenza. The therapeutic efficacy of rimantadine HCl in a naturally occurring influenza A₂ outbreak. *Am. J. Med. Sci.* **1969**, *257*, 328–335. [[CrossRef](#)] [[PubMed](#)]
8. Rosenthal, K.S.; Sokol, M.S.; Ingram, R.L.; Subramanian, R.; Fort, R.C. Tromantadine: Inhibitor of early and late events in *herpes simplex virus* replication. *Antimicrob. Agents Chemother.* **1982**, *22*, 1031–1036. [[CrossRef](#)] [[PubMed](#)]
9. Burstein, M.E.; Serbin, A.V.; Khakhulina, T.V.; Alyмова, I.V.; Stotskaya, L.L.; Bogdan, O.P.; Manukchina, E.E.; Jdanov, V.V.; Sharova, N.K. Inhibition of HIV-1 replication by newly developed adamantane-containing polyanionic agents. *Antiviral Res.* **1999**, *41*, 135–144. [[CrossRef](#)]
10. El-Emam, A.A.; Al-Deeb, O.A.; Al-Omar, M.A.; Lehmann, J. Synthesis, antimicrobial, and anti-HIV-1 activity of certain 5-(1-adamantyl)-2-substituted thio-1,3,4-oxadiazoles and 5-(1-adamantyl)-3-substituted aminomethyl-1,3,4-oxadiazoline-2-thiones. *Bioorg. Med. Chem.* **2004**, *12*, 5107–5113. [[CrossRef](#)] [[PubMed](#)]
11. Balzarini, J.; Orzeszko, B.; Mauri, J.K.; Orzeszko, A. Synthesis and anti-HIV studies of 2-adamantyl-substituted thiazolidin-4-ones. *Eur. J. Med. Chem.* **2007**, *42*, 993–1003. [[CrossRef](#)] [[PubMed](#)]
12. Balzarini, J.; Orzeszko-Krzesińska, B.; Maurin, J.K.; Orzeszko, A. Synthesis and anti-HIV studies of 2- and 3-adamantyl-substituted thiazolidin-4-ones. *Eur. J. Med. Chem.* **2009**, *44*, 303–311. [[CrossRef](#)] [[PubMed](#)]
13. Sun, S.Y.; Yue, P.; Chen, X.; Hong, W.K.; Lotan, R. The synthetic retinoid CD437 selectively induces apoptosis in human lung cancer cells while sparing normal human lung epithelial cells. *Cancer Res.* **2002**, *62*, 2430–2436. [[PubMed](#)]
14. Jia, L.; Tomaszewski, J.E.; Hanrahan, C.; Coward, L.; Noker, P.; Gorman, G.; Nikonenko, B.; Protopopova, M. Pharmacodynamics and pharmacokinetics of SQ109, a new diamine-based antitubercular drug. *Br. J. Pharmacol.* **2005**, *144*, 80–87. [[CrossRef](#)] [[PubMed](#)]
15. Protopopova, M.; Hanrahan, C.; Nikonenko, B.; Samala, R.; Chen, P.; Gearhart, J.; Einck, L.; Nacy, C.A. Identification of a new antitubercular drug candidate, SQ109, from a combinatorial library of 1,2-ethylenediamines. *J. Antimicrob. Chemother.* **2005**, *56*, 968–974. [[CrossRef](#)] [[PubMed](#)]
16. Villhauer, E.B.; Brinkman, J.A.; Naderi, G.B.; Burke, B.F.; Dunning, B.E.; Prasad, K.; Mangold, B.L.; Russell, M.E.; Hughes, T.E. 1-(3-Hydroxy-1-adamantyl)aminoacetyl-2-cyano-(S)-pyrrolidine: A potent, selective, and orally bioavailable dipeptidyl peptidase IV inhibitor with antihyperglycemic properties. *J. Med. Chem.* **2003**, *46*, 2774–2789. [[CrossRef](#)] [[PubMed](#)]
17. Augeri, D.J.; Robl, J.A.; Betebenner, D.A.; Magnin, D.R.; Khanna, A.; Robertson, J.G.; Wang, A.; Simpkins, L.M.; Taunk, P.; Huang, Q.; et al. Discovery and preclinical profile of saxagliptin (BMS-477118): A highly potent, long-acting, orally active dipeptidyl peptidase IV inhibitor for the treatment of type 2 diabetes. *J. Med. Chem.* **2005**, *48*, 5025–5037. [[CrossRef](#)] [[PubMed](#)]
18. Anagnostis, P.; Katsiki, N.; Adamidou, F.; Athyros, V.G.; Karagiann, A.; Kita, M.; Mikhailidis, D.P. 11-Beta-Hydroxysteroid dehydrogenase type 1 inhibitors: Novel agents for the treatment of metabolic syndrome and obesity-related disorders. *Metabolism* **2013**, *62*, 21–33. [[CrossRef](#)] [[PubMed](#)]
19. Olson, S.; Aster, S.D.; Brown, K.; Carbin, L.; Graham, D.W.; Hermanowski-Vosatka, A.; LeGrand, C.B.; Mundt, S.S.; Robbins, M.A.; Schaeffer, J.M.; et al. Adamantyl triazoles as selective inhibitors of 11β-hydroxysteroid dehydrogenase type 1. *Bioorg. Med. Chem. Lett.* **2005**, *15*, 4359–4362. [[CrossRef](#)] [[PubMed](#)]
20. Cheng, H.; Hoffman, J.; Le, P.; Nair, S.K.; Cripps, S.; Matthews, J.; Smith, C.; Yang, M.; Kupchinsky, S.; Dress, K.; et al. The development and SAR of pyrrolidine carboxamide 11β-HSD1 inhibitors. *Bioorg. Med. Chem. Lett.* **2010**, *20*, 2897–2902. [[CrossRef](#)] [[PubMed](#)]
21. Cott, J.S.; Choormun, J. 11β-Hydroxysteroid dehydrogenase Type 1 (11β-HSD-1) inhibitors in development. In *New Therapeutic Strategies for Type-2 Diabetes, Small Molecule Approaches*; Jones, R.N., Ed.; RSC: Cambridge, UK, 2012; pp. 109–133.
22. Thoma, G.; Streiff, M.B.; Kovarik, J.; Glickman, F.; Wagner, T.; Beerli, C.; Zerwes, H. Orally bioavailable isothioureas block function of the chemokine receptor CXCR4 in vitro and in vivo. *J. Med. Chem.* **2008**, *51*, 7915–7920. [[CrossRef](#)] [[PubMed](#)]
23. Berlin, M.; Boyce, C.W.; Ruiz, M.L. Histamine H₃ receptor as a drug discovery target. *J. Med. Chem.* **2011**, *54*, 26–53. [[CrossRef](#)] [[PubMed](#)]
24. Dai, H.; Fu, Q.; Shen, Y.; Hu, W.; Zhang, Z.; Timmerman, H.; Leurs, R.; Chen, Z. The histamine H₃ receptor antagonist clobenpropit enhances GABA release to protect against NMDA-induced excitotoxicity through the cAMP/protein kinase A pathway in cultured cortical neurons. *Eur. J. Pharmacol.* **2007**, *563*, 117–123. [[CrossRef](#)] [[PubMed](#)]

